Video Article

Determination of Lipid Raft Partitioning of Fluorescently-tagged Probes in Living Cells by Fluorescence Correlation Spectroscopy (FCS)

Catherine Marquer[1], Sandrine Lévêque-Fort[2,3], Marie-Claude Potier[1]

[1]Centre de Recherche de l'Institut du Cerveau et de la Moelle Épinière, Hôpital de la Pitié-Salpêtrière

[2]Institut des Sciences Moléculaires d'Orsay, Université Paris-Sud

[3]Centre de Photonique Biomédicale du Centre Laser, Université Paris-Sud

Correspondence to: Catherine Marquer at catherine.marquer@upmc.fr

URL: https://www.jove.com/video/3513
DOI: doi:10.3791/3513

Keywords: Cellular Biology, Issue 62, Lipid rafts, plasma membrane, diffusion times, confocal microscopy, fluorescence correlation spectroscopy (FCS)

Date Published: 4/6/2012

Citation: Marquer, C., Lévêque-Fort, S., Potier, M.C. Determination of Lipid Raft Partitioning of Fluorescently-tagged Probes in Living Cells by Fluorescence Correlation Spectroscopy (FCS). *J. Vis. Exp.* (62), e3513, doi:10.3791/3513 (2012).

Abstract

In the past fifteen years the notion that cell membranes are not homogenous and rely on microdomains to exert their functions has become widely accepted. Lipid rafts are membrane microdomains enriched in cholesterol and sphingolipids. They play a role in cellular physiological processes such as signalling, and trafficking[1,2] but are also thought to be key players in several diseases including viral or bacterial infections and neurodegenerative diseases[3].

Yet their existence is still a matter of controversy[4,5]. Indeed, lipid raft size has been estimated to be around 20 nm[6], far under the resolution limit of conventional microscopy (around 200 nm), thus precluding their direct imaging. Up to now, the main techniques used to assess the partition of proteins of interest inside lipid rafts were Detergent Resistant Membranes (DRMs) isolation and co-patching with antibodies. Though widely used because of their rather easy implementation, these techniques were prone to artefacts and thus criticized[7,8]. Technical improvements were therefore necessary to overcome these artefacts and to be able to probe lipid rafts partition in living cells.

Here we present a method for the sensitive analysis of lipid rafts partition of fluorescently-tagged proteins or lipids in the plasma membrane of living cells. This method, termed Fluorescence Correlation Spectroscopy (FCS), relies on the disparity in diffusion times of fluorescent probes located inside or outside of lipid rafts. In fact, as evidenced in both artificial membranes and cell cultures, probes would diffuse much faster outside than inside dense lipid rafts[9,10]. To determine diffusion times, minute fluorescence fluctuations are measured as a function of time in a focal volume (approximately 1 femtoliter), located at the plasma membrane of cells with a confocal microscope (**Fig. 1**). The auto-correlation curves can then be drawn from these fluctuations and fitted with appropriate mathematical diffusion models[11].

FCS can be used to determine the lipid raft partitioning of various probes, as long as they are fluorescently tagged. Fluorescent tagging can be achieved by expression of fluorescent fusion proteins or by binding of fluorescent ligands. Moreover, FCS can be used not only in artificial membranes and cell lines but also in primary cultures, as described recently[12]. It can also be used to follow the dynamics of lipid raft partitioning after drug addition or membrane lipid composition change[12].

Video Link

The video component of this article can be found at https://www.jove.com/video/3513/

Protocol

1. Calibration of the FCS Setup

1. Start the confocal microscope, lasers, computers, incubator for temperature and CO_2 control.
2. Make sure the SPAD (Single Photon Avalanche Diode) is on and the fluorescence filter inside the SPAD is well suited to your sample. Check that the SPAD is synchronized in time. Beware to only start your FCS software once your SPAD settings are ready for acquisition.
3. Prepare a fresh solution of cholera toxin-Alexa488 diluted in PBS to reach a concentration of 1 µg/ml (17.5 nM).
4. Optimize confocal imaging of the solution using internal detection of the microscope.
5. Switch to point scanning mode and choose a point in the solution sample. Make sure the duration of the laser illumination is long enough to perform your FCS acquisitions (> 5 minutes).
6. Switch to external detection by the SPAD and to the FCS software. Monitor your fluorescence signal and make sure it is well suited to the SPAD (enough signal but no saturation, 10 000 to 50 000 counts/s is fine). If necessary, modify z position, gain and/or laser power to achieve correct fluorescence signal.

7. Acquire 10 sets of 30 seconds measurements. Acquisition time should be optimized for your sample (compromise between the best sampling and photobleaching problems).
8. Analyze your data (see step 4) to ensure that you have an auto-correlation curve corresponding to one fluorescent species diffusing in solution (equation in **Fig. 2**) and that the diffusion time obtained after fitting is correct (approximately 0.2 ms) (**Fig. 3**).

2. Staining of Living Cells with Lipid Rafts Marker

1. Plate HEK293 cells on 8-well Labteks coated with poly-L-lysine (1mg/ml) the day before imaging to make sure that their adhesion is correct. Use medium without phenol red to ensure there is no perturbation of the fluorescence signal.
2. Wash cells twice with HBSS (Hank's Buffered Salt Solution).
3. Add cholera toxin-Alexa488 (1 µg/ml)/BSA (0,1 %) in 500 µl HBSS to the cells for 30 minutes at 37 °C. Cholera toxin will bind to ganglioside GM1, known to be preferentially partitioned in lipid rafts.
4. Wash cells twice with HBSS (Hank's Buffered Salt Solution).

3. FCS Data Acquisition on Living Cells

1. Place the stained cells on the microscope stage. Make sure temperature and CO_2 conditions are optimal otherwise this may lead to artefacts in diffusion times.
2. Optimize confocal imaging of a cell of interest using internal detection of the microscope (**Fig. 4**).
3. Switch to point scanning mode and choose a point in the plasma membrane of the cell of interest. Perform 1-2 live images of the cell to make sure the cell is not moving during acquisition.
4. Switch to external detection by the SPAD and to the FCS software. Monitor your fluorescence signal and make sure it is well suited to the SPAD (enough signal but no saturation, 10 000 to 50 000 counts/s is fine). If necessary, modify z position, gain and/or laser power to achieve correct fluorescence signal. If this is not enough, you may consider changing staining conditions.
5. Acquire 10 samples of 30 seconds measurements. As most cells are auto-fluorescent, you may see a decrease in fluorescence during the first acquisitions, due to auto-fluorescence fading.

4. FCS Data Analysis

1. Set the correlation interval and generate auto-correlation curves with the FCS software. The correlation interval will typically range from the shortest resolvable lag time up to the longest time possible (as the statistics of the measurement becomes more and more inadequate when maximum correlation time approaches total acquisition time, the maximum lag time is limited to 80% of the acquisition time on the Picoquant software).
2. For each sample, export files corresponding to fluorescence fluctuations and auto-correlation as a function of time.
3. Use a data analysis and fitting software such as Origin Pro to import the files.
4. For each sample, make sure there is no photobleaching during acquisition ie the fluorescence stays stable during the 30 seconds. Discard any measure displaying photobleaching as this may cause artificial longer diffusion times.
5. Check that the shape of the remaining FCS curves is correct (see **Fig 5**). Determine the mean FCS curve.
6. Fit the curve with the appropriate mathematical model (**Fig. 2**). This fit will give you the diffusion time(s) and the proportion of molecules diffusing with this (ese) diffusion time(s).

5. Representative Results

An example of an FCS calibration with a cholera toxin-Alexa488 solution is shown in **Figure 3**. After checking that individual measures of fluorescence as a function of time did not show any photobleaching (**Figure 3A**), individual and mean FCS curves were calculated. Mean FCS curves were fitted with equations corresponding to various diffusion models (examples in **Figure 2**). The parameter classically considered to determine the quality of a fit is the coefficient of determination R^2. The closer R^2 is to 1, the better the fit. In this case, the most accurate model to fit the mean FCS curve is the one describing a population of fluorescent molecules diffusing freely in three dimensions (**equation 1 in Figure 2 and Figure 3B**). The diffusion time derived from the fit is 0.32 ms. Residuals from curve-fitting (**Figure 3C**) and R^2 factor (0.99906) give an estimate of the quality of the fit.

An example of FCS analysis for cholera toxin-Alexa488 stained HEK293 cells is shown in **Figure 5**. The multiphasic mean FCS curve shape reveals the existence of populations of fluorescent molecules with different diffusion times. The best fit for this curve corresponds to a model with three populations of fluorescent probes: two with an hindered diffusion (diffusion in two dimensions as in the membrane plane) and one freely diffusing in three dimensions (**equation 2 in Figure 2 and Figure 5**). This latter population corresponds to fluorescent molecules moving outside of the membrane plane, i.e., either binding or unbinding to their membrane targets, reaching the membrane through the secretion or recycling pathway, or leaving the membrane by endocytosis. The two diffusion times at the membrane, corresponding to cholera toxin bound to GM1, were 2 ms (25% of molecules), corresponding to diffusion outside of lipid rafts, and 75 ms (50% of molecules), corresponding to diffusion in lipid rafts. Please note that any photobleaching during acquisition will lead to artificial longer diffusion times thus possibly creating a bias towards localization of GM1 in lipid raft domains.

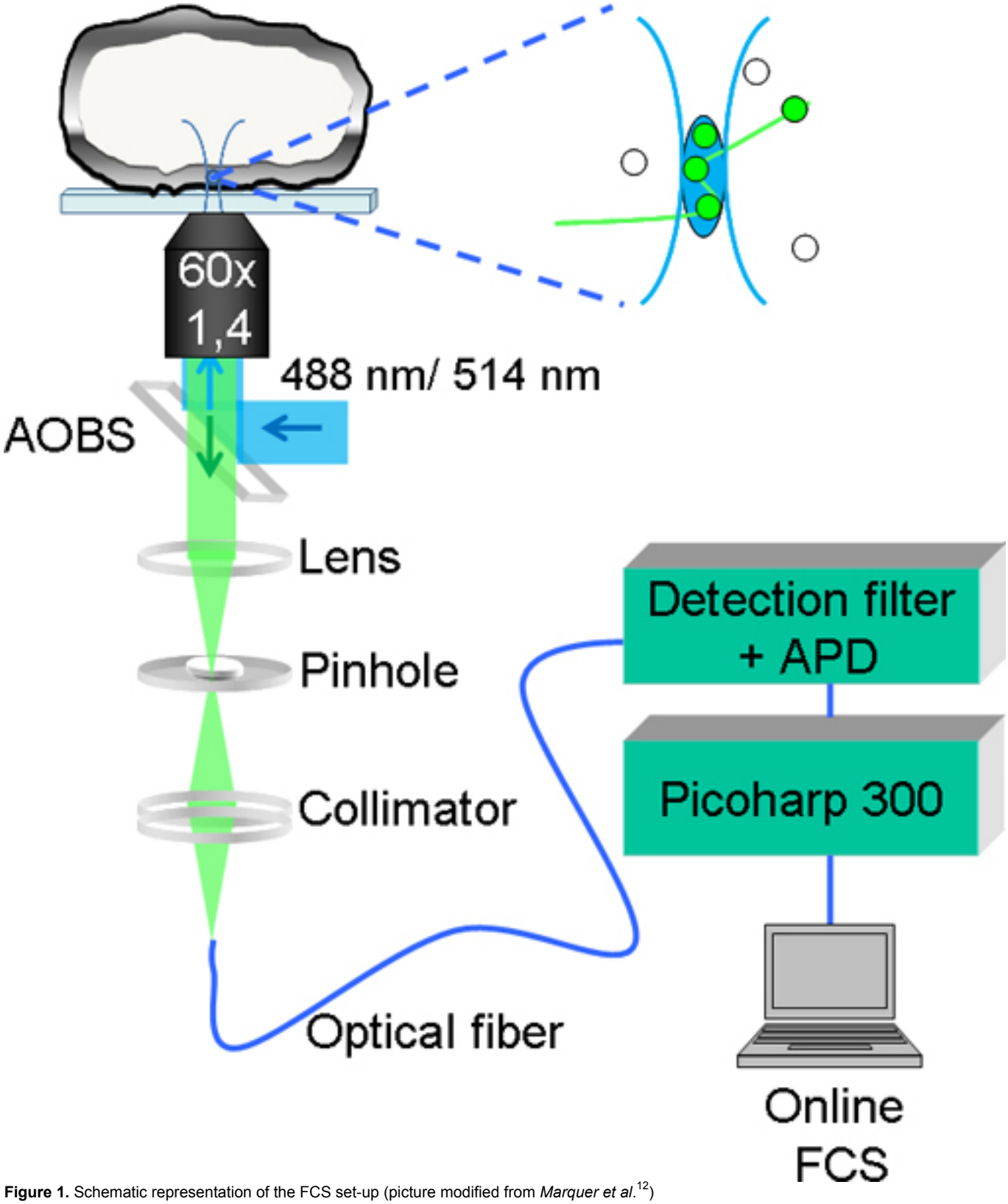

Figure 1. Schematic representation of the FCS set-up (picture modified from *Marquer et al.*[12])

Equation 1:

For 3D free diffusion of one population (e.g. fluorophore solution):

$$G(t) = (Neff)^{-1} \times (1 + t / \tau_{diff})^{-1} \times (1 + t / S^2 \tau_{diff})^{-1/2}$$

Equation 2:

For 3D free diffusion of one population and two populations moving in 2D in the mem
(e.g. cholera toxin-Alexa488, APP-YFP or Bace1-GFP in neurons):

$$G(t) = (Neff)^{-1} \times \left[\begin{array}{l} F_{3D} \times (1 + t / \tau_{diff3D})^{-1} \times (1 + t / S^2 \tau_{diff3D})^{-1/2} + F_{2D1} \times (1 + t / \tau_{diff2D1})^{-1} \\ + (1 - F_{3D} - F_{2D1}) \times (1 + t / \tau_{diff2D2})^{-1} \end{array} \right] + C$$

With t representing time, Neff the average number of fluorescent molecules in the ef
measurement volume, τ_{diff} the diffusion time of a given population, S the structure pa
which characterizes the shape of the detection volume, C the constant offset due to
fluorescence fluctuations and F the fraction of molecules of a given population.
S is based on the point spread function (PSF) determined for the objective and micro
used for acquisition and is fixed during fitting.

Figure 2. Example of diffusion models and corresponding equations used to fit autocorrelation curves. The structure parameter S can be written as $S = z_0/w_0$ with z_0 the effective focal radius along the optical axis at $1/e^2$ intensity and w0 the effective lateral focal radius at $1/e^2$ intensity. These values can be extracted from a classical point spread function (PSF) measurement.

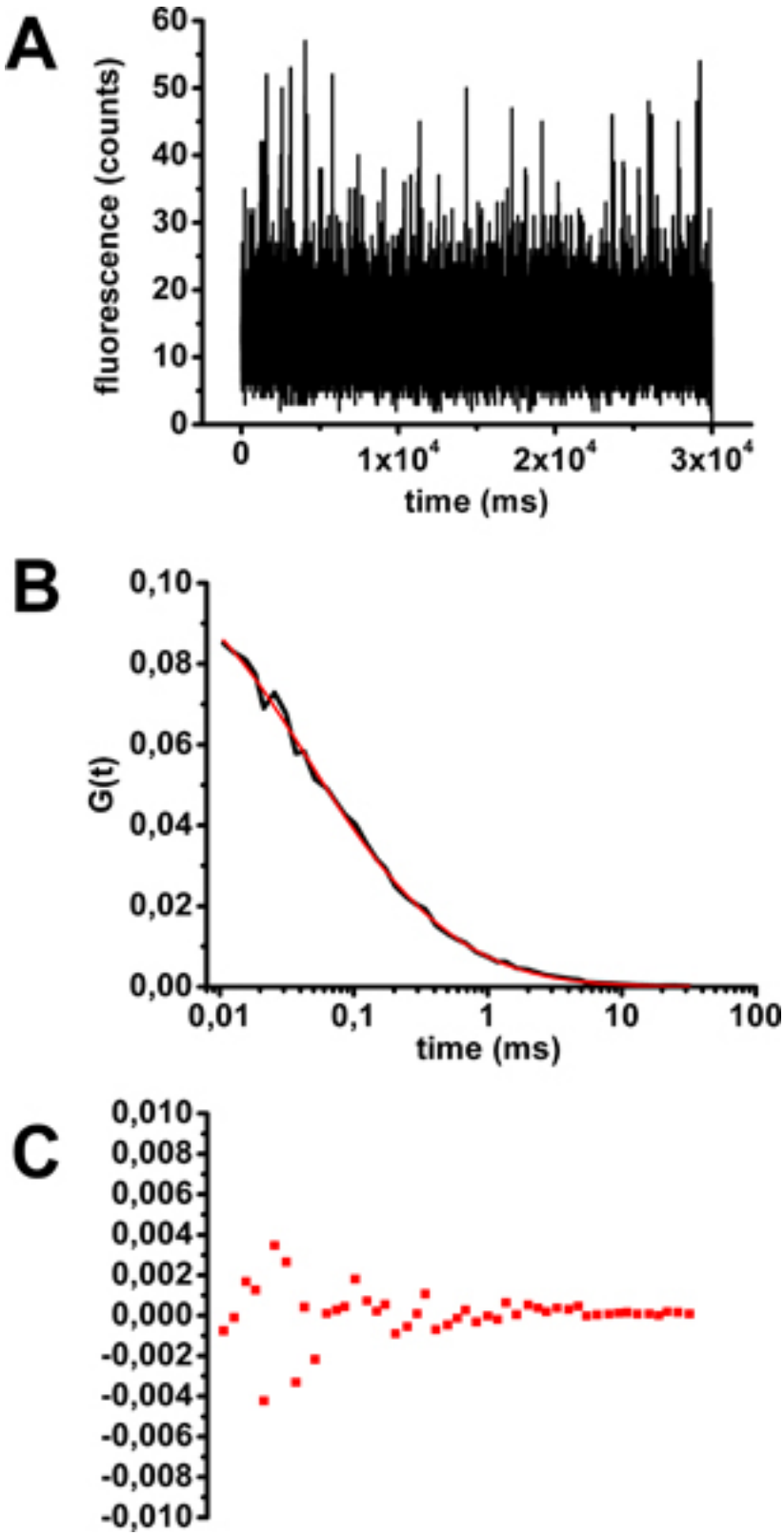

Figure 3. Assessment of diffusion time of cholera toxin-Alexa488 in solution for FCS calibration. A) Fluorescence fluctuation as a function of time for a representative example of a 30 seconds acquisition. B) Mean autocorrelation curve obtained from 10 samples of 30 seconds acquisition fitted with equation 1 (see Figure 2).C) Residuals from curve fitting.

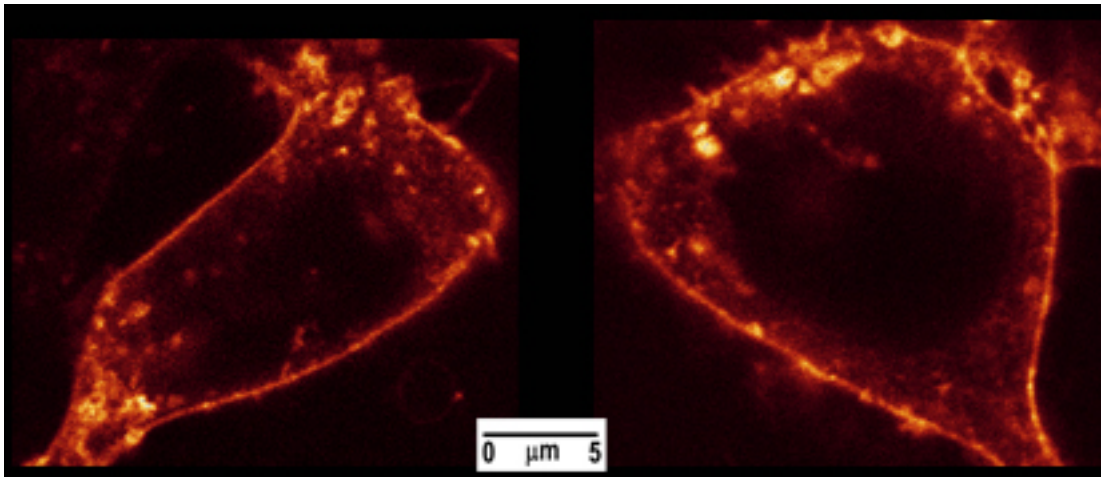

Figure 4. HEK-293 cell stained with cholera toxin-Alexa488. Cells were imaged on an SP5 confocal microscope (Leica Microsystems, Wetzlar, Germany) with the internal 488nm laser line. Fluorescence was collected with a x60 plan apochromat oil immersion objective between 500 and 650 nm.

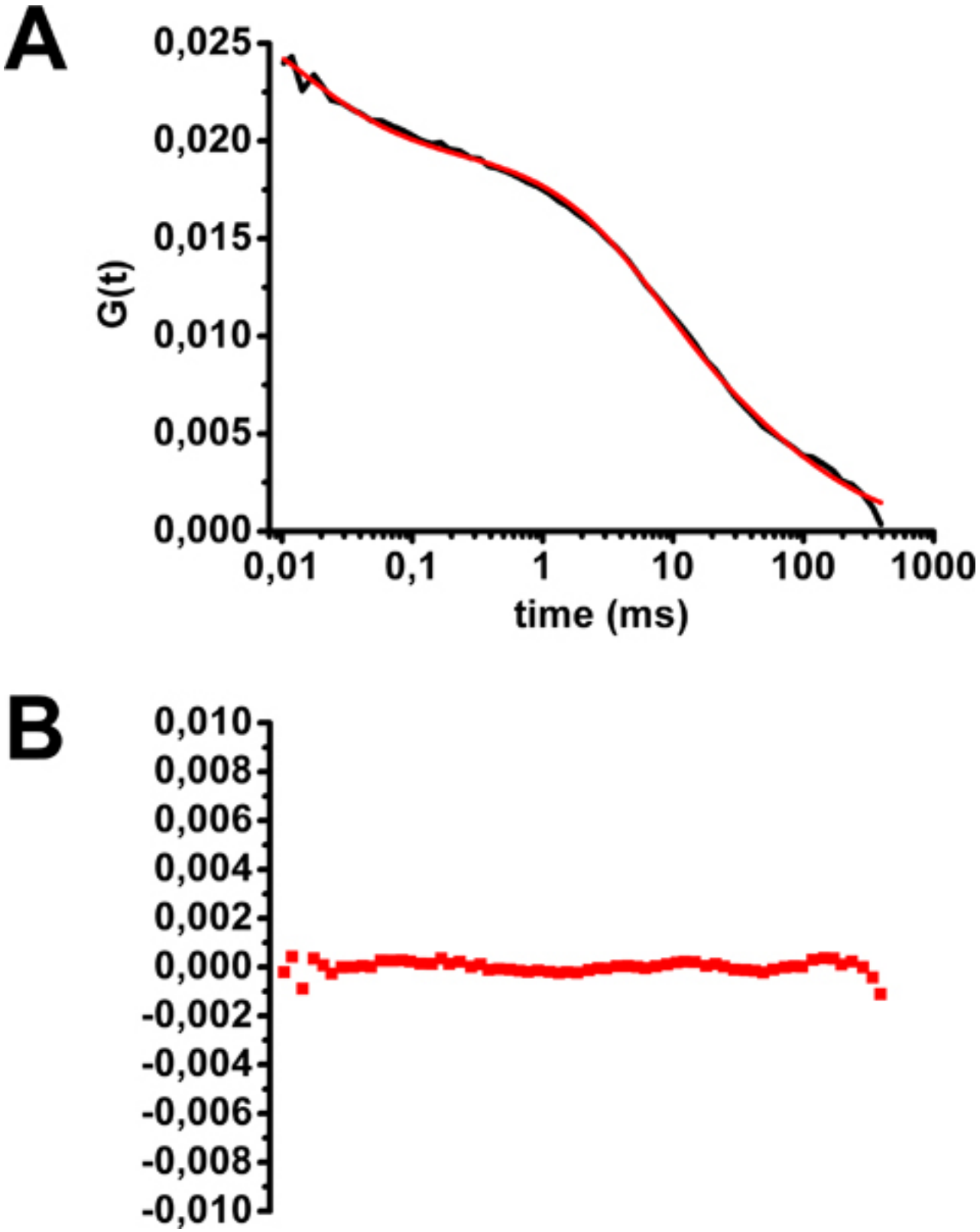

Figure 5. Assessment of diffusion time of cholera toxin-Alexa488 at the plasma membrane of HEK293 cells. A) Mean autocorrelation curve fitted with equation 2 (see **Figure 2**). B) Residuals from curve fitting. (modified from *Marquer et al.*[12])

Discussion

The FCS method presented here enables a sensitive and rapid analysis of the lipid raft partitioning of fluorescent probes of interest in living cells. FCS combines the accuracy of localization of confocal microscopy with the sensitivity of single photon counting. The main difference between FCS and standard biochemical techniques is that FCS enables the absolute determination of the lipid rafts partition of the target and not the relative partition as is the case for DRMs isolation or co-patching.

Acquisition of FCS data takes approximately 5 minutes (10 acquisitions of 30 seconds) for each sample and is thus quite rapid as compared to usual biochemical techniques. This rapidity makes it possible to follow in time the perturbation in lipid raft partitioning that may result from drug addition. However, analysis of autocorrelation curves can be a bit tricky as the different models for fitting have to be browsed through to determine the most accurate one. Moreover, photobleaching during acquisition has to be avoided as this may lead to artifacts.

Here we describe an example where we can delineate the lipid raft partitioning of a lipid: ganglioside GM1 (**Fig. 5**). Such a study would not have been possible with standard biochemical procedures which can only be applied to proteins. FCS is not limited to lipids though and can also be used for proteins, either tagged with a fluorescent ligand (e.g. transferrin-Alexa555 binds to the transferrin receptor, known to be located outside of rafts[9]) or expressed as a fusion with a fluorescent protein (e.g. APP-YFP or Bace1-GFP[9], two key protein players in Alzheimer's disease). It can thus be used for a wide range of targets. Further, FCS can be implemented not only in cell lines, as described here, but also in primary cultures[9].

Concerning cholera toxin, you should keep in mind that it has a tendency to aggregate GM1 in pentamers, thus creating membrane micro-domains that can be different from native lipid rafts. That is why you cannot use colocalisation with cholera toxin to determine if your protein of interest is inside or outside of rafts. Nevertheless, membrane proteins, such as APP-YFP and Bace1-GFP, diffuse in lipid rafts with diffusion times of 60-80 ms[9], very similar to what was observed with cholera toxin (75 ms). Thus cholera toxin can be used to calibrate your set-up and check that you can differentiate between fast and slow diffusion times.

FCS is also suited for many other applications[13,14] such as determination of the oligomerisation state of a protein[15] or ligand/receptor pharmacological studies[16]. It can also be coupled to other microscopy techniques such as Total Internal Reflection Fluorescence (TIRF)[17,18] or STimulated Emission Depletion (STED)[19]. Indeed, STED-FCS allows an even more accurate determination of lipid raft partitioning[19] but up to now, STED microscopy is still costly and thus not widespread.

The main limits of FCS are the need for low concentrations of fluorophores (in the nanomolar range) and fast diffusion times so that fluorophores will not photobleach before leaving the excitation volume. Complementary techniques to assess the diffusion of proteins include FRAP (Fluorescence Recovery After Photobleaching) and ICS (Image Correlation Spectroscopy) techniques (reviewed in [20]).

In FRAP, a high intensity laser beam is used to photobleach a region of a cell and the recovery of fluorescence after photobleaching is then monitored. This recovery comes from the diffusion of fluorophores from non-bleached areas to the bleached area. Thus the diffusion times can be extracted from the recovery kinetics. FRAP can be used with high concentrations of fluorophores and can access large range of diffusion times, thus making it complementary to FCS. FRAP has been used to assess whether a fluorophore was majoritarily inside or outside of rafts[21,22] but it is still a rather bulk method to quantify the proportion of fluorophores diffusing inside or outside rafts in the area of interest.

ICS is an imaging analog of FCS, in which spatial correlation is calculated pixel by pixel for a given image[23]. It has the advantage to be amenable to the study of slowly diffusing fluorescent probes but is limited to 2D analysis. This limit was overcome by the development of ICS termed Spatio-Temporal ICS (STICS)[24]. STICS enables spatio-temporal correlation of fluorescent probes on a stack of images and is thus a powerful technique though it requires a lot of computational implementation and has a lower time resolution than FCS. In fact, both ICS and STICS are limited to process much slower than the acquisition time of one image frame. Another extension of ICS called raster ICS (RICS)[25,26] enables the analysis of fast diffusion process by taking advantage of the raster scan mode available on most commercial confocal microscopes. RICS is versatile as it can be used for a large diffusion range (from µs to ms) but its implementation (scanning parameters, data processing) can be cumbersome. We did not find many papers in the literature reporting the use of ICS and its derived techniques to study lipid rafts[27-29].

Disclosures

No conflicts of interest declared.

Acknowledgements

This work was supported by a grant from Agence Nationale de la Recherche (ChoAD). We are also grateful to the Fondation ICM (Institut du Cerveau et de la Moelle) for their financial support.

References

1. Brown, D.A. & London, E. Functions of lipid rafts in biological membranes. *Annu. Rev. Cell Dev. Biol.* **14**, 111-136 (1998).
2. Simons, K. & Gerl, M.J. Revitalizing membrane rafts: new tools and insights. *Nat. Rev. Mol. Cell Biol.* **11**, 688-699 (2010).
3. Simons, K. & Ehehalt, R. Cholesterol, lipid rafts, and disease. *J. Clin. Invest.* **110**, 597-603 (2002).
4. Munro, S. Lipid rafts: elusive or illusive? *Cell.* **115**, 377-388 (2003).
5. Shaw, A.S. Lipid rafts: now you see them, now you don't. *Nat. Immunol.* **7**, 1139-1142 (2006).

6. Pralle, A., Keller, P., Florin, E.L., Simons, K., & Horber, J.K. Sphingolipid-cholesterol rafts diffuse as small entities in the plasma membrane of mammalian cells. *J. Cell Biol.* **148**, 997-1008 (2000).
7. Brown, D.A. & London, E. Structure and function of sphingolipid- and cholesterol-rich membrane rafts. *J. Biol Chem.* **275**, 17221-17224 (2000).
8. Sharma, P., Sabharanjak, S., & Mayor, S. Endocytosis of lipid rafts: an identity crisis. *Semin. Cell Dev. Biol.* **13**, 205-214 (2002).
9. Kahya, N., Scherfeld, D., Bacia, K., Poolman, B., & Schwille, P. Probing lipid mobility of raft-exhibiting model membranes by fluorescence correlation spectroscopy. *J. Biol. Chem.* **278**, 28109-28115 (2003).
10. Bacia, K., Scherfeld, D., Kahya, N., & Schwille, P. Fluorescence correlation spectroscopy relates rafts in model and native membranes. *Biophys J.* **87**, 1034-1043 (2004).
11. Kim, S.A., Heinze, K.G., & Schwille, P. Fluorescence correlation spectroscopy in living cells. *Nat. Methods.* **4**, 963-973 (2007).
12. Marquer, C., *et al.* Local cholesterol increase triggers amyloid precursor protein-Bace1 clustering in lipid rafts and rapid endocytosis. *FASEB J.* **25**, 1295-1305 (2011).
13. Tian, Y., Martinez, M.M., & Pappas, D. Fluorescence correlation spectroscopy: a review of biochemical and microfluidic applications. *Appl. Spectrosc.* **65**, 115A-124A (2011).
14. Haustein, E. & Schwille, P. Fluorescence correlation spectroscopy: novel variations of an established technique. *Annu. Rev. Biophys. Biomol. Struct.* **36**, 151-169 (2007).
15. Ilien, B., *et al.* Pirenzepine promotes the dimerization of muscarinic M1 receptors through a three-step binding process. *J. Biol. Chem.* **284**, 19533-19543 (2009).
16. Lieto, A.M., Cush, R.C., & Thompson, N.L. Ligand-receptor kinetics measured by total internal reflection with fluorescence correlation spectroscopy. *Biophys. J.* **85**, 3294-3302 (2003).
17. Thompson, N.L., Burghardt, T.P., & Axelrod, D. Measuring surface dynamics of biomolecules by total internal reflection fluorescence with photobleaching recovery or correlation spectroscopy. *Biophys. J.* **33**, 435-454 (1981).
18. Thompson, N.L. & Steele, B.L. Total internal reflection with fluorescence correlation spectroscopy. *Nat. Protoc.* **2**, 878-890 (2007).
19. Eggeling, C., *et al.* Direct observation of the nanoscale dynamics of membrane lipids in a living cell. *Nature.* **457**, 1159-1162 (2009).
20. Kolin, D.L. & Wiseman, P.W. Advances in image correlation spectroscopy: measuring number densities, aggregation states, and dynamics of fluorescently labeled macromolecules in cells. *Cell Biochem. Biophys.* **49**, 141-164 (2007).
21. Shvartsman, D.E., Kotler, M., Tall, R.D., Roth, M.G., & Henis, Y.I. Differently anchored influenza hemagglutinin mutants display distinct interaction dynamics with mutual rafts. *J. Cell Biol.* **163**, 879-888 (2003).
22. White, R., *et al.* Holin triggering in real time. *Proc. Natl. Acad. Sci. U.S.A.* **108**, 798-803 (2011).
23. Petersen, N.O., Hoddelius, P.L., Wiseman, P.W., Seger, O., & Magnusson, K.E. Quantitation of membrane receptor distributions by image correlation spectroscopy: concept and application. *Biophys. J.* **65**, 1135-1146 (1993).
24. Hebert, B., Costantino, S., & Wiseman, P.W. Spatiotemporal image correlation spectroscopy (STICS) theory, verification, and application to protein velocity mapping in living CHO cells. *Biophys. J.* **88**, 3601-3614 (2005).
25. Digman, M.A., *et al.* Measuring fast dynamics in solutions and cells with a laser scanning microscope. *Biophys. J.* **89**, 1317-1327 (2005).
26. Digman, M.A., *et al.* Fluctuation correlation spectroscopy with a laser-scanning microscope: exploiting the hidden time structure. *Biophys. J.* **88**, L33-36 (2005).
27. Nohe, A., Keating, E., Fivaz, M., van der Goot, F.G., & Petersen, N.O. Dynamics of GPI-anchored proteins on the surface of living cells. *Nanomedicine.* **2**, 1-7 (2006).
28. Semrau, S. & Schmidt, T. Particle image correlation spectroscopy (PICS): retrieving nanometer-scale correlations from high-density single-molecule position data. *Biophys. J.* **92**, 613-621 (2007).
29. Bates, I.R., *et al.* Membrane lateral diffusion and capture of CFTR within transient confinement zones. *Biophys. J.* **91**, 1046-1058 (2006).

